

Research Article

Promoting differentiation of human adipose mesenchymal stem cells into oligodendrocyte-like cells and neuron-like cells through coculture on decellularized sciatic nerves

Carlos I. Valencia-Salgado^{1,†} , Selene Jacobo-Arreola^{1,†} , Salvador L. Said-Fernandez¹ , Adolfo Soto-Dominguez² , Alberto Camacho-Morales¹ , Herminia G. Martinez-Rodriguez¹ , Humberto Rodriguez-Rocha², Paulina Delgado-Gonzalez¹ , Adriana G. Quiroz-Reyes¹ , Jose F. Islas¹ and Elsa N. Garza-Treviño^{1,*} 

¹ Departamento de Bioquímica y Medicina Molecular, Facultad de Medicina, Universidad Autónoma de Nuevo León, León, Mexico; carlosvalenciasalgado@gmail.com (CIVS); selenej26@gmail.com (SJA); salvador.said@gmail.com (SLSF); herminia-mar@gmail.com (HGMR); alberto.camachomr@uanl.edu.mx (ACM); paulina.delgadogn@uanl.edu.mx (PDG); adri.quiroz.ry@gmail.com (AGQR); jislas.me0117@uanl.edu.mx (JFI)

² Departamento de Histología, Facultad de Medicina, Universidad Autónoma de Nuevo León, León, Mexico; adolfo.soto-dmn@uanl.edu.mx (ASD); humberto.rodriguezrc@uanl.edu.mx (HRR)

[†] these authors contributed equally to this work

* Correspondence: egarza.nancy@gmail.com (ENGT)

Abstract: We evaluated cell markers of oligodendrocyte-like cells (OLC) and neuron-like cells (NLC) differentiation from human adipose tissue-derived mesenchymal stem cells (hADSCs) cocultured on decellularized sciatic nerves. OLC and NLC were incubated at a 10:1 ratio with decellularized rat nerves. We estimated the percentage of myelin basic protein (MBP)- and neurofilament protein (NFP)-positive cells. OLC and NLC cocultures showed an increase in positive cells for MBP and proteolipid protein (PLP) markers. Oligodendrocytes and neurons cocultured with sciatic nerve scaffolds promoted myelination by OLC within 3 days, which remained stable for at least 21 days. We propose a reproducible experimental strategy to promote sciatic nerve myelination by coculturing hADSCs-derived OLC and NLC in nerve scaffolds.

Keywords: scaffolds; adipose tissue-derived mesenchymal stem cells; oligodendrocyte-like cells; sciatic nerve

Received: 22 December 2021; Accepted: 27 February 2022; Published: 15 April 2022

Introduction

Neurons and glia integrate the major cell type components of the central nervous system (CNS). Neurons promote the reception and transmission of nerve impulses, whereas glia (including astrocytes, oligodendrocytes, microglia, and ependyma-like cells) coordinates metabolic efficiency, mechanical support, and neuronal protection [1].

Oligodendrocyte precursor cells (OPC) proliferate and differentiate into myelin-forming oligodendrocytes, which promote myelination and also efficiently support neuronal axons by wrapping them with multiple layers of their myelin-rich plasma membranes, maximizing and maintaining nerve impulse conduction [2]. Disruption of the oligodendrocyte-axon unit occurs in Alzheimer, demyelinating diseases, and traumatic injuries, resulting in low myelin production. Recent works propose that dead oligodendrocytes can be replenished from the adult OPC pool. Any loss of myelin can be regenerated during remyelination. These changes can prevent axonal degeneration and restore neuronal function [3]. There are two major myelin proteins: myelin basic protein (MBP) and proteolipid protein (PLP). They compose up to 80% of the total myelin proteins [4].

Myelin-associated glycoprotein (MAG) and myelin oligodendrocyte glycoprotein (MOG) contribute to myelin stability [5]. Selective molecular and cellular characterization of myelination is still not fully un-

derstood. However, *in vitro* assays addressing oligodendrocyte and myelin biology have provided important advances in the field. Many mitogens and trophic factors, such as platelet-derived growth factor (PDGF), basic fibroblast growth factor (bFGF), triiodothyronine (T3), progesterone, insulin-like growth factor 1, and transferrin, among others, promote OPC proliferation, maturation, and survival, which correlate with the A2B5 and neuron-gial antigen 2 (NG2) markers [6–11]. Mature myelinating oligodendrocytes sequentially express galactosylceramidase (GalC), PLP, MBP, MAG, and MOG. Surface ligands, secreted molecules, and axonal activity control the myelination of individual axons by oligodendrocytes [12].

In vitro models have documented the efficacy of transplantation in multifunctional three-dimensional (3D) scaffolds, stem cell-derived cell lineages, metabolic substrates, and vitamin cofactor exposure or selective genomic-cell differentiation into an injured area, as potential therapeutic strategies favoring neuronal regeneration and improvement of motor function [13]. Autologous peripheral nerve transplantation into a chronic spinal cord injury (SCI) has shown clinical improvements in motor sensitivity and function in patients avoiding graft rejection. Recent reports showed that autologous peripheral nerve grafts, along with a chitosan-laminin scaffold and bone marrow-derived mesenchymal stem cells, promoted axonal regeneration [14]. Chemical methods can help designing acellular peripheral nerve scaffolds that provide structural support and beneficial properties for cell growth, allowing axonal regeneration, including high availability, low immunogenicity, and an intact 3D structure resembling the nerve tissue [15]. Because of the lack of effective therapies that promote myelination by oligodendrocytes, we propose a model that improves the myelinating activity of oligodendrocyte-like cells (OLC) through coculture with neuron-like cells (NLC) on decellularized sciatic nerves as scaffolds.

Materials and Methods

Isolation and culture of human adipose tissue-derived mesenchymal stem cells (hADSCs)

Adipose tissue was obtained from patients who underwent voluntary liposuction and signed informed consent. Adipose tissue was collected into two tubes of 50 mL each. It was washed three times in sterile 0.1 mM phosphate-buffered saline (PBS) solution and twice in PBS supplemented with 2.5 µg/mL amphotericin B and 100 µg/mL gentamicin (PBSs). Adipose tissue was cut into small portions using a scalpel and digested with collagenase I (0.04 g/mL) under magnetic stirring at 37 °C for 90 min. The digested tissue was stored in a conical 50 mL centrifuge tube. Cells were washed, suspended with 5 mL PBS, and centrifuged at 5,000 rpm for 10 min; they were then resuspended in 5 mL of Dulbecco's Modified Eagle Medium (DMEM)/F12 (GIBCO-BRL, Grand Island, NY, USA) supplemented with 10% fetal bovine serum (FBS, GIBCO-BRL), 50 µg/mL gentamicin, and 2.5 µg/mL amphotericin (DMEM/F12s). Adipocytes were seeded in 25 cm² cell culture flasks and incubated at 37 °C, 5% CO₂, until they reached 80% confluence. Adherent cells were detached by incubation with a 0.25% trypsin-EDTA solution (GIBCO-BRL), washed with PBS, and seeded again as required in five 25 cm² flasks with 5 mL of DMEM/F12s, supplemented as described above.

hADSCs characterization by immunocytochemistry

After reaching the third passage and 80% confluence, adherent cells were detached using a 0.25% trypsin-EDTA solution. Viable cells were quantified through the Trypan Blue exclusion assay. Then, 1×10⁵ viable cells were seeded per well on 4-well plates (Nunc 177399 Lab-Tek ChamberSlid, ThermoScientific) and incubated at 37 °C and 5% CO₂ until they reached 80% confluence. Monolayers of cultured cells were then washed with PBS, fixed with 500 µL 1:1 (v/v) methanol-acetone solution for 20 min at 4 °C, washed again with PBS, and stored at 4 °C until use. hADSCs were characterized with typical markers of mesenchymal stem cell lineage, by immunocytochemistry, using the anti-CD34 and anti-CD90 (1:200, USBiological, Salem, Massachusetts, USA) and anti-CD105 (1:10, Abcam, Cambridge, UK, C2446-55) monoclonal antibodies, followed by the mouse and rabbit specific HRP/DAB detection system (Abcam, Cambridge, UK, No. ab64264), according to the manufacturer's instructions. Slides were analyzed with a Nikon Eclipse 50i microscope, equipped with a Sight DS-2MV XCite120 EXFO camera.

Morphometric analysis of hADSCs

We analyzed six random images to determine the percentage of CD90⁺, CD34⁺ and CD105⁺ immunoreactivity, using the Nikon system (Nikon, Konan, Minato-ku, Tokyo, Japan). The quantitative signal was determined with the ENIS-elements BR 2.30 software (ENIS-Elements B12 Model 2.30, Nikon). The mean number of CD90⁺, CD34⁺ and CD105⁺ cells × 100/total number of cells was determined.

Differentiation of hADSCs into OLC

hADSCs in the fourth passage were differentiated into OLC following the procedure described by Abbaszadeh and colleagues [16]. Briefly, 1×10^5 cells were inoculated in 25 cm² flasks in DMEM/F12 medium supplemented with 2% DMSO (Sigma-Aldrich, St. Louis, MO, USA), 50 µg/mL gentamicin, and 2.5 µg/mL amphotericin, for 24 h. To promote hADSCs differentiation into OLC, the medium was replaced by DMEM/F12 supplemented with 15% FBS and 1 µM all-trans retinoic acid (ATRA) (Calbiochem, Merck KGaA Darmstadt, Germany), and incubated for 72 h. Then, the medium was replaced by DMEM/F12 supplemented with 10 ng/mL bFGF (Peprotech, Rocky Hill, NJ INC., USA), 5 ng/mL platelet-derived growth factor AA (PDGF-AA) (Peprotech INC., Rocky Hill, NJ, USA), and 200 ng/mL heregulin (Peprotech) for an additional 48 h. Complete differentiation was achieved by adding 35 ng/mL T3 (Sigma) to the medium and incubating for 48 h. Cultures were maintained in DMEM/F12 supplemented with 10 ng/mL bFGF, 5 ng/mL PDGF-AA, 35 ng/mL T3, and 200 ng/mL heregulin (DMEM/F12s). 3D culture of differentiated cells was performed using DMEM/F12s and Matrigel as an extracellular matrix (ECM) (1:4) and incubated at 37 °C, 5% CO₂, for 72 h. Cells were released from this matrix by incubation with 200 IU/mL collagenase I (Sigma-Aldrich, Mexico) for 4 h and gently mixed with a pipette.

Phenotypic and genomic characterization of OLC

OLC identity was confirmed by immunocytochemistry using MBP (1:250, Abcam, Cambridge, MA, USA) and PLP (1:100, Abcam, Cambridge, MA, USA) antibodies, two major and typical markers of mature oligodendrocytes. Also, histological sections of gray and white matter from a human brain were used as positive and negative controls. For genomic characterization of OLC, RNA was extracted with the RNeasy Lipid Tissue kit (Qiagen, CA, USA), following the manufacturer's directions. RNA integrity was verified by agarose gel electrophoresis, by confirming high quality and non-degraded RNA through the presence of 28S and 18S rRNA subunits. For each sample, 250 ng RNA were treated with DNase I (1U/µL, Invitrogen) according to the manufacturer's instructions, to remove DNA (2 µL DNase I per 10 µL RNA). RNA was then used to synthesize complementary DNA (cDNA) using a commercial kit of reverse transcriptase (Invitrogen) and following the instructions provided by the brand. All cDNA samples were diluted 1:5 prior to quantitative real-time PCR (qPCR) analysis.

Primers and qPCR of OLC markers

Genomic characterization of OLC was performed by analyzing the mRNA expression of seven representative genes from mature oligodendrocytes: 2',3'-cyclic-nucleotide 3'-phosphodiesterase (CNPase), oligodendrocyte transcription factor 2 (Olig2), MOG, O4, PDGFR- α , Nestin and NG2. End-point PCR primers were used: CNPase (523 bp) Fw 5'-AACTGACCCTCCCTTCCTGT-3', Rev 5'-GGTAAATAGCCCCAGCCTTC-3'; Olig2 (286 bp) Fw 5'-TAAAAGGCAGTTGCTGTGGA-3', Rev 5'-GACGCTACAAAGCCCAGTTT-3'; MOG (280 bp) Fw 5'-TTGGTGAGGGAAAGGTGACT-3', Rev 5'-TCAAAGTCCGGTGGAGATT-3'; O4 (348 bp) Fw 5'-CTACTGCTCTGGGTCCCAGG-3', Rev 5'-CTGCCACTGAACCGAGATGG-3'; PDGFR- α (116 bp) Fw 5'-CGCTTCCTGATATTGAGTGG-3', Rev 5'-TCGGGAGTGGATCTCCGTGA-3'; Nestin (388 bp) Fw 5'-TCCAGGAACGAAAATCAAG-3', Rev 5'-TAGAGACCTCCGTCGCTGTT-3'; NG2 (271 bp) Fw 5'-ACTGGCTAGGGGTGTCAATG-3', Rev 5'-TCCTCAAGGTCCTGCTGAGT-3'. Glyceraldehyde 3-phosphate dehydrogenase (GAPDH) was used as an internal control (470 bp): Fw 5'-CCATCACCATCTTCCAGGAGCG-3', Rev 5'-AAGGCCATGCCAGTGAGCTTC-3'. The conditions for the amplification of the GAPDH gene were 95 °C for 5 min, 30 cycles (94 °C for 1 min, 55 °C 1 min and 72 °C 1 min) and 72 °C for 6 min. For Nestin, Olig2, CNPase and MOG genes, the amplification conditions were: 95 °C for 5 min, 30 cycles (94 °C for 1 min, 58 °C for 1 min and 72 °C for 1 min) and 72 °C for 5 min. For PDGFR- α : 95 °C for 5 min, 30 cycles (94 °C for 1 min, 62 °C for 2 min and 72 °C for 2 min) and 72 °C for 5 min. For NG2: 95 °C for 5 min, 30 cycles (94 °C for 1 min, 60 °C for 1 min and 72 °C for 1 min) and 72 °C for 5 min. For O4: 95 °C for 5 min, 32 cycles (94 °C for 30 s, 55 °C for 30 s and 72 °C for 30 s) and 72 °C for 10 min. GoTaq Green Master Mix (Promega, Madison, WI, USA) was used. We also used hADSCs and brain tissue as negative and positive controls of OLC, respectively. Different RNA amounts (54-154 ng) were used to synthesize cDNA using a reverse transcriptase commercial kit (Invitrogen). Amplified products (250 ng) were loaded onto a 1% agarose gel, followed by electrophoresis at 90 V, stained with ethidium bromide, and visualized under ultraviolet light to determine qualitative genomic expression.

For the MBP gene, a 275 bp fragment was amplified using Fw 5'-CTGGGCAGCTGTTAGAGTCC-3' and Rev 5'-CTGTGGTTTGGAAACGAGGT-3' primers. For the PLP gene, a 247 bp fragment was amplified using Fw 5'-GGCGACTACAAGACCACCAT-3' and Rev 5'-AGGTGGTCCAGGTGTTGAAG-3' primers. Amplification was performed using standard qPCR conditions in the 7500 FAST Real-Time PCR Detection System (Applied Biosystems).

Differentiation of hADSCs into NLC

hADSCs in their fourth culture passage were induced to differentiate into NLC following the protocol reported by Jang and colleagues [17]. Briefly, 100,000 cells were seeded in 25 cm² flasks containing DMEM/F12 with 1% FBS, 100 ng/mL bFGF, 50 ng/mL gentamicin, and 2.5 µg/mL amphotericin B and incubated for 7 days. Cells were exposed to an induction medium containing 1% FBS, 100 ng/mL bFGF, 10 µM forskolin (Sigma-Aldrich, St. Louis, MO, USA), 50 µg/mL gentamicin, and 2.5 µg/mL amphotericin B in DMEM/F12 medium for the following 7 days. Neuronal identity was characterized by immunocytochemistry using anti-neurofilament protein (NFP) antibodies (1:2, Leica Biosystems). hADSCs and the C6 glioblastoma cell line were used as negative and positive controls, respectively.

OLC and NLC monolayer coculture

OLC and NLC were seeded at a 10:1 ratio (200,000/20,000) in 4-well plates of the Chamber Slide System. Each well contained 1000 µL of coculture medium, which consisted of DMEM/F12 medium supplemented with 1% FBS, 35 ng/mL T3, 100 ng/mL bFGF, 5 ng/mL PDGF, 200 ng/mL heregulin and 10 µM forskolin (DMEM/F12co). Cultures were incubated for 7 days at 37 °C, 5% CO₂, and the medium was replaced by fresh DMEM/F12co medium every third day. OLC and NLC were characterized by immunocytochemistry as described above. All assays were performed in triplicate.

Decellularization/demyelination of rat sciatic nerves

Sciatic nerves of Wistar rats were obtained following the ethics and safety guidelines for animal research. Sciatic nerves were cleaned and isolated from connective tissue. Nerves were cut into 20-mm long fragments and decellularized following the protocol described by García-Pérez and colleagues [18]. Briefly, sciatic nerves were cleaned with distilled sterile water and submerged in ultrapure water for 10 h. Water was replaced every 2 h; then, the nerves were submerged in a 3% Triton X-100 solution overnight, and then in a 4% sodium deoxycholate solution for the following 24 h. During all the procedures, the sciatic nerves were shaken at 500 rpm, and the sequence above was repeated for 15 days. Finally, decellularized nerves were cleaned one last time with ultrapure water, submerged in PBS, and stored at 4 °C until further use.

Morphological analysis of rat sciatic nerves

Decellularized sciatic nerves and controls (non-decellularized sciatic nerves) were fixed with 2.5% glutaraldehyde solution and stained with hematoxylin-eosin (H & E) to visualize cell nuclei. Masson's trichrome staining was used to visualize collagen I fibers (blue), contrasting with red cytoplasm and violet/brown nuclei. Immunohistochemistry against MBP (1:250, Abcam) was also performed to characterize the demyelination ratio.

Oligodendrocyte-neuron coculture in decellularized sciatic nerves

Decellularized sciatic nerves were softly and carefully injected with 50 µL cell suspension containing 1×10⁶ oligodendrocytes/mL and 1×10⁵ neurons/mL in DMEM/F12co. Sciatic nerves were seeded in 24-well plates and incubated in DMEM/F12co at 37 °C, 5% CO₂, for 3, 7, and 21 days. The medium was replaced every third day by fresh DMEM/F12co medium. After the incubation period, sciatic nerves were fixed with Carnoy's solution (6:3:1 (v/v) ethanol:acetic acid:chloroform) for 24 h and sectioned longitudinally (4 µM) using a microtome. The nerves were stained with H & E, and oligodendrocytes and neurons were identified by immunohistochemistry against MBP, PLP, and NFP. All experiments were performed in triplicate after every incubation.

Densitometry and statistical analysis

ImageJ and GraphPad Prism softwares were used to measure the density units (DUs) in the control and test nerves to make a subsequent comparative analysis. For the statistical analysis of the immunohistochemistry results, six randomized power fields of every slide were analyzed with the ImageJ software version v5, which was used to quantify the number of positively stained cells and the optical DUs. All data are presented as means ± SEM. All statistical analyses, including normality of data distribution testing, were performed using GraphPad Prism 7.01 and IBM SPSS version 22, and a corrected *p*-value < 0.05 was considered significant.

Results

Characterization of hADSCs, oligodendrocytes and neurons by immunocytochemistry

We selectively isolated mesenchymal stem cells from adipose tissue lipoaspirate. Primary culture cells from the lipoaspirates were 85% positive for both CD90 and CD105, and 90% positive for CD34, compared with the negative control (Fig. 1A-D). Adherent cells displayed a spindle shape, resembling the typical mesenchymal stem cell phenotype. Fig. 1G shows differentiated hADSCs displaying round and

voluminous cell bodies, integrating long and tiny multiple prolongations, suggestive of the oligodendrocyte-like appearance. Immunohistochemical characterization showed that, after differentiation into OLC, there was $22.26 \pm 5.12\%$ NFP expression, $13.36 \pm 7.25\%$ MBP expression, and $15.37 \pm 5.73\%$ PLP expression. Neither MBP nor PLP were detected in non-differentiated hADSCs, compared with the OLC (Fig. 1H). We also found that $76.8 \pm 10.4\%$ of hADSCs preserved the fibroblast-like morphology of the mesenchymal stem cell phenotype. The immunohistochemistry of the NFP marker in the control cells and neurons is shown in Fig. 1I-L.

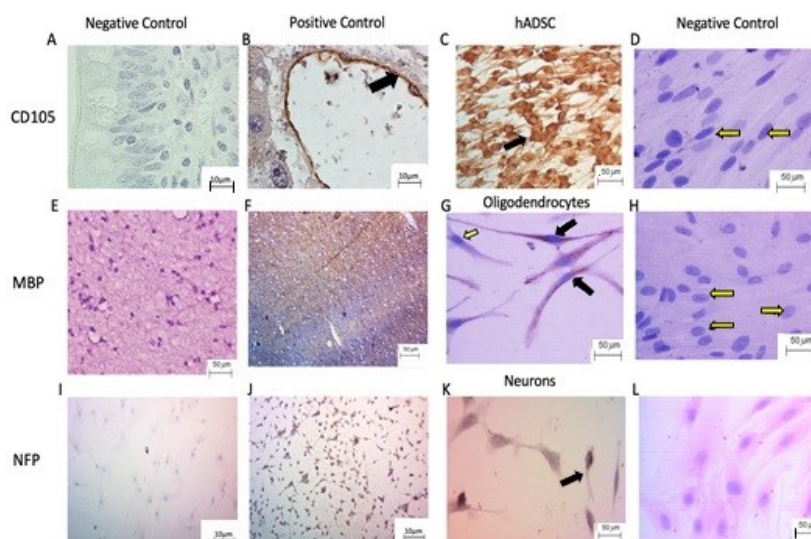


Figure 1. Morphological characterization and cell surface markers of hADSCs, oligodendrocytes, and neurons. (A) CD105-negatively stained jejunum. (B) CD105-positively stained central vein endothelium in the human liver. (C) hADSCs stained in the third passage, showing a typical mesenchymal stem cell phenotype. (D) Unstained hADSCs. (E) MBP-negatively stained white matter, processed with no primary antibody. (F) MBP-positively stained human brain tissue. (G) hADSCs differentiated into oligodendrocytes and stained with MBP. (H) hADSCs stained with the anti-MBP primary antibody. (I) NFP-negatively stained C6 cells, processed with no primary antibody. (J) NFP-positively stained C6 cells. (K) hADSCs differentiated into neurons and stained with anti-NFP primary antibody. (L) hADSCs stained with anti-NFP primary antibody. Black arrows show cells with positive signal (with brown color), and yellow arrows show cells with negative signal.

Molecular characterization of hADSCs-derived oligodendrocytes by qPCR

Qualitative RNA expression was shown for GAPDH, Nestin, Olig2, CNPase, MOG, PDGFR- α , NG2, and O4 (Fig. 2A). When compared to undifferentiated hADSCs, OLC differentiated from hADSCs show a significant increase in Nestin, CNPase, and PDGFR- α gene expression ($p < 0.05$) (Fig. 2B), supporting an early and late oligodendrocyte differentiation phenotype. Also, the expression of MBP and PLP genes was higher in OLC ($p < 0.05$) (Fig. 2C). There was no expression of Olig2, MOG, NG2, and O4 in differentiated cells (OLC).

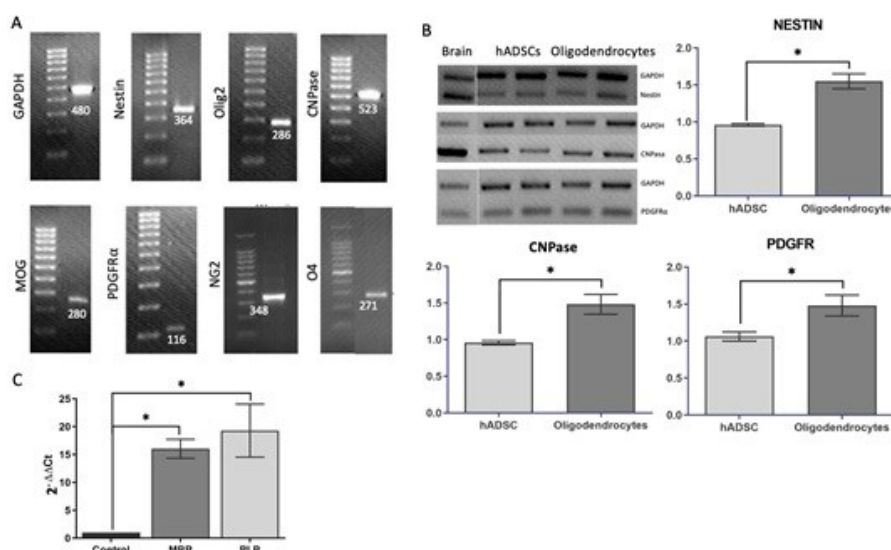


Figure 2. Expression levels of oligodendrocyte representative genes. (A) Agarose gels showing amplified PCR products of Nestin, Olig2, CNPase, MOG, PDGFR- α , NG2, O4 genes, and GADPH as a housekeeping gene. (B) Gene expression levels of Nestin, CNPase, and PDGFR- α in hADSCs, oligodendrocytes, and brain (positive control) (from three independent experiments, performed in triplicate). (C) Relative expression ($2^{-\Delta\Delta C_t}$) of MBP and PLP genes in cells treated to differentiate compared to untreated cells. Quantitative analysis of qPCR data using one-way ANOVA followed by the Bonferroni post-hoc test ($n = 2$, performed in triplicate). * $p < 0.05$.

OLC and NLC coculture

We characterized the differentiation of hADSCs into NLC. Figure 3A shows the phenotypic traits of NLC, displaying a pyramidal cell body with one or two long emerging prolongations and a dendrite-like appearance. Immunohistochemical analysis also confirmed that $10.50 \pm 4.49\%$ of cells were expressing NFP (Fig. 3D). We observed that hADSCs-derived oligodendrocytes and neurons could fully coexist and interact with each other, preserving the typical morphology and cell lineage identity at least 15 days post-differentiation (Fig. 3D-G). Notably, co-culturing oligodendrocytes-neurons dramatically increased cell differentiation markers, showing an increase in MBP-positive cells from $13.65 \pm 7.73\%$ to $81.54 \pm 8.26\%$, in PLP-positive cells from $15.37 \pm 5.73\%$ to $89.28 \pm 8.23\%$, and in NFP-positive cells from $10.50 \pm 4.49\%$ to $22.26 \pm 5.12\%$ (Fig. 3H). These data confirm that hADSCs-derived oligodendrocytes and neurons can coexist and interact with each other, favoring phenotypic and molecular differentiation profiles for each lineage.

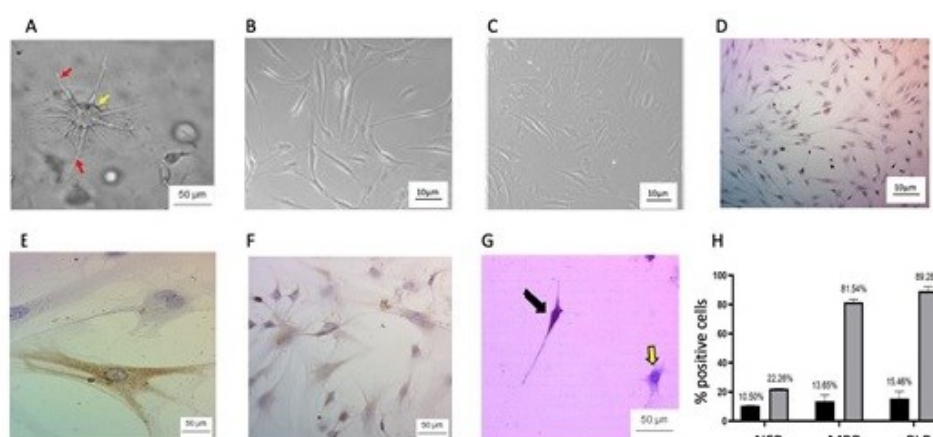


Figure 3. Morphological characterization and cell surface markers of oligodendrocytes and neurons in coculture, as observed under an inverted bright-field microscope. (A) hADSCs differentiate into oligodendrocytes (the yellow arrow shows the cell body and red arrows the cytoplasmic extensions). (B) hADSCs differentiate into neurons. (C) hADSCs. (D) Immunohistochemistry against MBP in oligodendrocytes in coculture with neurons (10 \times magnification). (E) Immunohistochemistry against NFP in neuron coculture with oligodendrocytes (40 \times magnification). (F) Positively stained MBP in oligodendrocyte coculture with neurons. (G) Positive staining for PLP (black arrow) in oligodendrocytes in coculture with neurons; the yellow arrow shows a negatively stained cell. (H) Percentage of cells positively stained for NFP, MBP, and PLP markers for oligodendrocytes alone (black bars), and in coculture with neurons (gray bars).

Decellularized sciatic nerves as scaffolds

Rat sciatic nerves were decellularized through exposure to 3% Triton X-100 and 4% sodium deoxycholate solutions for 15 days (see Materials and Methods). We confirmed that decellularized sciatic nerves exhibited absence of cell nuclei (Fig. 4A, B). No morphological changes were observed on collagen fibers in decellularized nerves compared with non-decellularized sciatic nerves (Fig. 4A, B), confirming that the decellularization protocol does not affect the ECM. Of note, myelin staining in decellularized nerves was dramatically decreased (Fig. 4C, D). These data are compatible with a reliable experimental protocol of sciatic nerve decellularization that efficiently depletes myelin from nerves, keeping the ECM unaltered and providing a proper scaffold.

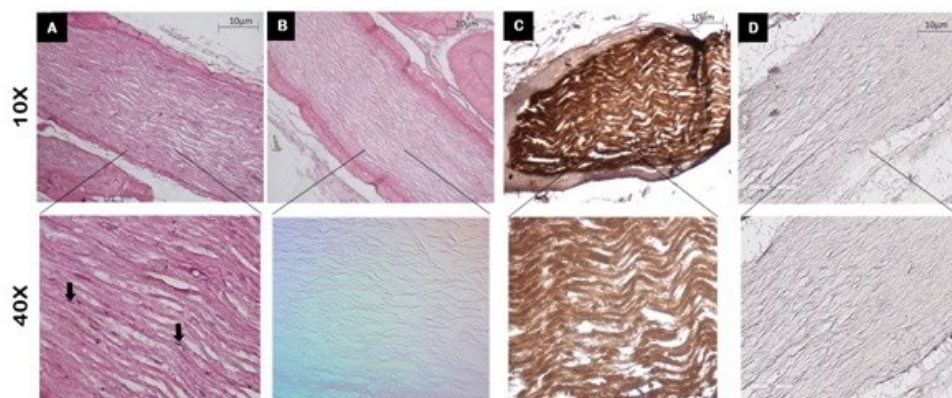


Figure 4. Decellularization of rat sciatic nerves. (A) H & E staining of non-decellularized sciatic nerves; black arrows denote cell nuclei. (B) H & E staining of the decellularized sciatic nerve; absence of black arrows denotes the absence of cell nuclei. (C) Immunohistochemistry of non-decellularized sciatic nerves against MBP, confirming myelin integrity. (D) Immunohistochemistry of demyelinated sciatic nerves against MBP, confirming myelin absence.

OLC and NLC coculture using the decellularized nerves as a scaffold

DAPI-stained decellularized sciatic nerves exhibited absence of cell nuclei and remnants of genetic material (Fig. 5A). Scaffold recellularization by co-culturing hADSCs-derived OLC and NLC shows full and homogeneously conserved DAPI-stained nuclei resembling OLC and NLC (Fig. 5A, B), confirming proper cell implantation inside the sciatic nerve. Also, time-dependent decellularized/demyelinated longitudinal scaffold tracts substantially ablated MBP synthesis to 0.47 ± 0.14 DUs by days 3, 7, and 21 (Fig. 5J-L), compared with control scaffolds showing preservation of MBP staining to 74.3 ± 6.3 DUs values (Fig. 5D-F). Notably, recellularization of scaffolds by the coculture of OLC and NLC substantially recovered MBP synthesis, showing 8.9 ± 0.88 DUs by day 3 ($p < 0.0001$) (Fig. 5C, G), 7.34 ± 0.11 DUs by day 7 (Fig. 5C, H), and 5.10 ± 0.11 DUs by day 21 ($p < 0.0001$) (Fig. 5C, I), when compared with decellularized/demyelinated scaffolds (Fig. 5C, J-L). The morphological appearance of myelin by day 3 shows an irregular distribution and becomes stable, acquiring a tract-like arrangement resembling control sciatic nerve tracts, which are preserved by day 21 (Fig. 5C).

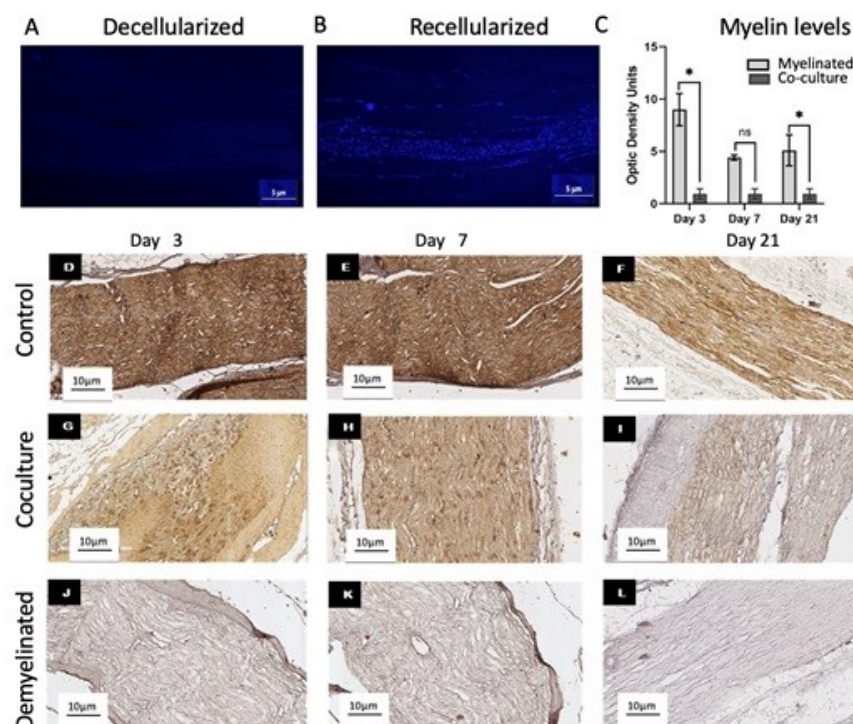


Figure 5. Recellularization of sciatic nerves with hADSCs-derived oligodendrocytes and neurons. (A) Decellularized and (B) recellularized sciatic nerve with oligodendrocytes and neurons stained with DAPI (4 \times magnification). (C) DUs of immunohistochemistry against MBP denote myelin levels; nerve without decellularization as a control (D-F), recellularized with oligodendrocytes and neurons (G-I) and decellularized (J-L) sciatic nerve by days 3, 7, and 21 (15 \times magnification). ns, not significant; * $p < 0.05$.

Discussion

Diseases of the central and peripheral nervous systems remain a challenge for clinical therapeutics. Major neurodegenerative diseases involve damage in oligodendrocyte-myelin and axon-neuron interactions. Scaffold assistance in cell therapy from hADSCs-derived cells might be an ideal source for treatment, based on their cell specificity, abundance, and availability [19,20]. In contrast to the classical stem cell therapeutic approaches, fully differentiated cells might integrate mature functional dynamics, create higher intercellular crosstalk at the cell-cell junction, and efficiently communicate with host cells [21]. *In vitro* differentiation of stem cells into other specific cell lineages will decrease the potency of these cells and increase the risk of tumor development [22].

Previous studies have shown that hADSCs actively differentiate into selective cell identities, including ectodermal, mesodermal, and endodermal lineages. Their differentiation into neurons and glial cells has also been widely explored. In this work, we differentiated hADSCs into oligodendrocytes with the method reported by Abbaszadeh and colleagues [16], and successfully achieved 81% bone marrow stromal cell transdifferentiation into OLC. Our results show that hADSCs-derived cells display a typical oligodendrocyte morphology in two-dimensional (2D) and 3D matrices, along with PDGFR- α and CNPase gene expression; however, maturation markers (MBP and PLP) were expressed in < 15% of cells. Recently, Zhou and co-workers demonstrated that mesenchymal stromal cells from human bone marrow with hADSCs had higher growth factor expression, promoting axonal growth and less demyelination in a SCI murine model [23]. Additional reports have shown that stem cells, such as spermatogonia stem cells, endometrial stromal cells, mouse induced pluripotent stem cells (iPSCs), and human iPSCs, can also differentiate into oligodendrocytes, reporting > 80% of cells expressing Olig2, which, along with the PDGFR- α gene, resembles the expression signature of OPC based on the MBP and glial fibrillary acidic protein (GFAP) genes [13,21,24–27]. The coculture and the oligodendrocyte medium contain PDGF, which, through PDGFR, leads to a rapid increase in the proportion of oligodendrocyte precursors. However, we did not use different concentrations, so it is not an inducer of differentiation, and we did not detect Olig2 expression in OLC, potentially because Olig2 expression defines the OPC state. Olig2 expression is dependent on T3 concentration. Throughout the duration of our study and with the T3 concentrations used, Olig2 was not detectable. We believe that the detection of Olig2 may require higher concentrations than those assayed in this work. We also evaluated the differentiation percentage of OLC using immunohistochemistry of MBP as a protein marker of mature oligodendrocytes, associated with myelination. Furthermore, we differentiated NLC using the protocol by Jang and co-workers [28]. Cells exhibited neuron-like morphology in 2D cultures and expressed the NFP marker, which efficiently confirms the presence of the major structural protein in the axonal network of neurons. Other markers that have been proposed for the identification of the maturation of oligodendrocytes and neurons are MBP, MAG, MOG, GalC and enolase 2, neuron-specific enolase (NSE), neuronal nuclear protein (NeuN), microtubule-associated protein 2 (MAP2), beta-III tubulin and growth associated protein 43 (GAP-43), but they were not evaluated in this work [3].

In a recent work, a 1:1 ratio of glial cells to neurons was shown in brain, but the posterior gray matter of the human spinal cord within the T8-T11 vertebral region was in the 11:1 to 13:1 range. This is the main area where damage occurs in patients with SCI [29]. Our work proposed a simple method that improves myelin expression of oligodendrocytes by coculturing OLC and NLC at a 10:1 ratio, exposed to FBS and growth factors such as trans-retinoic acid, T3, bFGF, PDGF, heregulin, and forskolin, in short culture periods. Our results demonstrated an increase in MBP immunoreactivity in 80% of the cells after seven days of coculture. Furthermore, we preserved the mutual interplay between oligodendrocytes and neurons as cell monolayers, denoting a typical 2D organization. Some authors have suggested that a 2D culture cannot precisely allow cell interactions to reproduce functional cell dynamics [30]. 3D structures, such as organoid methodologies or scaffolds, are required to achieve this goal [13,31].

Growth factors, such as bFGF and forskolin, which are not normally present in the oligodendrocyte differentiation medium, were added to the coculture medium. In turn, bFGF was added to the coculture medium at concentrations 10-fold higher than those usually used to differentiate oligodendrocytes using the protocol by Abbaszadeh and colleagues [16], as the fibroblast growth factor (FGF)/fibroblast growth factor receptor (FGFR) pathway plays a central role in the cell cycle of oligodendrocytes and their progenitors. Furthermore, it has been found that it could be a target to improve myelination and increase OLC differentiation. *In vivo* studies have shown that FGFR2 ablation in oligodendrocytes, but not FGFR1 signaling, attenuates myelin gene expression and myelin growth. As it was recently demonstrated, FGFR2 might play an important role in the reception and transmission of FGF signals, potentially presented by axons, to promote myelin growth [32]. In future studies, it would be interesting to explore if this mechanism applies to myelination using different bFGF concentrations in a coculture medium.

Another growth factor used in the culture medium was forskolin, which activates cyclic adenosine monophosphate (cAMP) synthesis, leading to the activation of neuroprotective signal cascades, and has been reported to regulate neuronal specification and to promote axonal regeneration. Both FGF2 and forskolin are FDA-approved reagents. Therefore, they may be involved in the clinical setting [33]. The culture medium was tested on both oligodendrocytes and neurons alone, which, in turn, allowed the conclusion that NLC and OLC, in combination with coculture media, enhance marker detection. In Fig. 3A, we show

oligodendrocytes with classic morphology in 3D culture, as compared with previous reports [34]; however, evidence of cell interaction and functionality is needed. We tested the differentiation of the coculture of OLC and NLC in decellularized rat sciatic nerves as scaffolds based on this proposal.

Acellular scaffolds are designed by selective chemical methods to provide structural support for cell growth, allowing axonal regeneration, high availability, low immunogenicity, and an intact 3D structure resembling nervous tissue [35–37]. The sciatic nerve, when used as a scaffold, can provide a more favorable environment for cell survival, as well as a trophic support for cells. A recent study showed that this environment was not fully favored, as researchers used a fully decellularized scaffold, preserving the ECM only, but not growth factors that would have helped promoting further cellular differentiation [38]. Among its advantages, this technology provides unlimited availability, low immunogenicity, and an intact 3D structure, similar to that of nerve tissue [39]. It was important to eliminate all cell remnants and to determine the basal levels of myelin in decellularized nerves in order to assess the potential of the OLC and NLC coculture and growth factors. We performed sciatic nerve decellularization by exposing the nerve to 3% Triton X-100 and 4% sodium deoxycholate solutions for 15 days [18]. We successfully produced a stable and defined scaffold that lacked cell bodies, as evidenced by the absence of DAPI staining and immunohistochemistry against MBP [40]. Chemical decellularization has been shown to variably remove growth factors from tissues and cells, which might limit cell differentiation and proliferation [36]. While some reports have documented that decellularization by chemical treatments can preserve remnants of growth factors that increase cell growth, we did not evaluate if changes in growth factors were affected or promoted in our experimental design [41]. These changes could be a workable aim for future experimental approaches [42,43]. Finally, one of the most significant contributions of our work is the positive increase in myelination of the scaffold upon coculturing OLC and NLC. After three days of coculturing, we detected an increase in MBP immunoreactivity in the decellularized sciatic nerve. We may expect that the results observed with OLC and NLC will be the maximum amount of myelin detected, as demonstrated on 2D culture. It was important to determine the distribution of each type of cell within the scaffold. However, it was difficult to detect NLC due to their low percentage in the scaffold.

OPC are susceptible to oxidative stress, directly influencing oligodendrocyte differentiation. Hence, changes in oligodendroglial function in response to differences in oxygen concentrations may also be mediated via hypoxia-inducible factor 1 α (HIF-1 α). In recent studies, in OLN93 cells (oligodendroglia cell line derived from primary rat brain glial cultures) under 5% O₂, HIF-1 α knockdown decreased the expression of MBP and CNPase, similar to that observed at 21% O₂ [44]. Other authors have shown that oxygen deprivation for 48 h does not significantly change MBP expression of differentiated oligodendrocytes; however, chronic hypoxia may induce myelin loss and neurodegeneration [45]. As expected, MBP expression shows a time-dependent decrease from day 3 to day 21. We propose that this decrease is due to a low concentration of growth factors and/or oxygenation in the culture medium and the scaffold, since it is tentative to expect a lack of infiltration into the tissue [46]. However, it would be interesting to measure HIF-1 α levels in future studies, to ascertain the role it plays in cell differentiation.

Previous work has shown that IPS-derived OPC could rescue a mouse model of hypomyelination that required over 120 days [47]. Additionally, it was also shown that an injectable peripheral nerve matrix can improve cell transplantation efficacy in the repair of SCI by using Schwann cells [48,49]. According to the authors, peripheral nerve, as an experimental model, provides generous support for spinal cord survival and myelination, axon growth, and locomotor recovery in rats [48]. Other reports propose that allografts of decellularized nerves could be used to connect and direct axonal growth after SCI, and are a key element in future clinical applications [50]. This evidence supports our current experimental work, underlining the advantages of scaffolds from decellularized nerves based on their accessibility and biocompatibility with resident cell lineages. In any case, a greater understanding and comprehension of the scaffold's biology and its interaction with oligodendrocytes and neurons in an *in vivo* model is required to ensure the absence of an immunogenic response in the host and the functionality in the cell microenvironment under vascular flow. Based on our experimental evidence, for future studies, it is necessary to evaluate other components that align axon growth and to analyze electrical conduction to validate the functionality of scaffold myelination.

In conclusion, we established a model to enhance the myelinating activity of OLC using NLC, growth factors, and nerves as scaffolds.

Acknowledgments

Special thanks to Sergio Lozano for reviewing this manuscript.

Author Contributions

CIVS performed coculture experiments, analyzed and discussed the results. SJA helped in the protocol of differentiation into oligodendrocytes. SLSF and HGMR designed the experiments, performed the literature analysis and acquired and managed the funding. ASD helped in the standardization of immunohistochemistry and with the fluorescence microscope software. ACM wrote, analyzed, and corrected the manuscript. HRR performed histological tissue processing. PDG analyzed and discussed the results.

AGQR performed statistical analysis and graphic design. JFI contributed to the experimental design, analyzed, and corrected the manuscript. ENGT participated in the experimental design, literature analysis, discussion of results and wrote the manuscript. All authors read and approved the final manuscript.

Conflicts of interest

The authors declare no competing interests.

Ethics statement

This project was authorized by the Ethics Committee of the UANL Medical School and University Hospital (registration no. BI14-005).

References

- Lloyd, A.F.; Miron, V.E. The Pro-Remyelination Properties of Microglia in the Central Nervous System. *Nat. Rev. Neurol.* **2019**, *15*, 447–458.
- Simons, M.; Nave, K.A. Oligodendrocytes: Myelination and Axonal Support. *Cold Spring Harb. Perspect. Biol.* **2016**, *8*, 1–16, doi:10.1101/cshperspect.a020479.
- Kuhn, S.; Gritti, L.; Crooks, D.; Dombrowsky, Y. Oligodendrocytes in Development, Myelin Generation and Beyond. *Cells* **2019**, *8*, doi:10.1016/j.coms.2016.10.001.
- Foerster, S.; Hill, M.F.E.; Franklin, R.J.M. Diversity in the Oligodendrocyte Lineage: Plasticity or Heterogeneity? *Glia* **2019**, *67*, 1–9, doi:10.1002/glia.23607.
- Peschl, P.; Bradl, M.; Höftberger, R.; Berger, T.; Reindl, M. Myelin Oligodendrocyte Glycoprotein: Deciphering a Target in Inflammatory Demyelinating Diseases. *Front. Immunol.* **2017**, *8*.
- Santos, A.K.; Vieira, M.S.; Vasconcellos, R.; Goulart, V.A.M.; Kihara, A.H.; Resende, R.R. Decoding Cell Signalling and Regulation of Oligodendrocyte Differentiation. *Semin. Cell Dev. Biol.* **2019**, *95*, 54–73.
- Lee, J.Y.; Petratos, S. Thyroid Hormone Signaling in Oligodendrocytes: From Extracellular Transport to Intracellular Signal. *Mol. Neurobiol.* **2016**, *53*, 6568–6583.
- Jure, I.; De Nicola, A.F.; Labombarda, F. Progesterone Effects on Oligodendrocyte Differentiation in Injured Spinal Cord. *Brain Res.* **2019**, *1708*, 36–46, doi:10.1016/j.brainres.2018.12.005.
- Wrigley, S.; Arafa, D.; Tropea, D. Insulin-like Growth Factor 1: At the Crossroads of Brain Development and Aging. *Front. Cell. Neurosci.* **2017**, *11*, 14, doi:10.3389/fncel.2017.00014.
- Cheli, V.T.; Correale, J.; Paez, P.M.; Pasquini, J.M. Iron Metabolism in Oligodendrocytes and Astrocytes, Implications for Myelination and Remyelination. *ASN Neuro* **2020**, *12*, 175909142096268, doi:10.1177/1759091420962681.
- Abbaszadeh, H.A.; Tiraihi, T.; Delshad, A.R.; Saghedizadeh, M.; Taheri, T.; Kazemi, H.; Hassoun, H.K. Differentiation of Neurosphere-Derived Rat Neural Stem Cells into Oligodendrocyte-like Cells by Repressing PDGF- α and Olig2 with Triiodothyronine. *Tissue Cell* **2014**, *46*, 462–469, doi:10.1016/j.tice.2014.08.003.
- Marisca, R.; Hoche, T.; Agirre, E.; Hoodless, L.J.; Barkey, W.; Auer, F.; Castelo-Branco, G.; Czopka, T. Functionally Distinct Subgroups of Oligodendrocyte Precursor Cells Integrate Neural Activity and Execute Myelin Formation. *Nat. Neurosci.* **2020**, *23*, 363–374, doi:10.1038/s41593-019-0581-2.
- Marton, R.M.; Miura, Y.; Sloan, S.A.; Li, Q.; Revah, O.; Levy, R.J.; Huguenard, J.R.; Paşca, S.P. Differentiation and Maturation of Oligodendrocytes in Human Three-Dimensional Neural Cultures. *Nat. Neurosci.* **2019**, *22*, 484–491, doi:10.1038/s41593-018-0316-9.
- Amr, S.M.; Gouda, A.; Koptan, W.T.; Galal, A.A.; Abdel-Fattah, D.S.; Rashed, L.A.; Atta, H.M.; Abdel-Aziz, M.T. Bridging Defects in Chronic Spinal Cord Injury Using Peripheral Nerve Grafts Combined with a Chitosan-Laminin Scaffold and Enhancing Regeneration through Them by Co-Transplantation with Bone-Marrow-Derived Mesenchymal Stem Cells: Case Series of 14 Patient. *J. Spinal Cord Med.* **2014**, *37*, 54–71, doi:10.1179/2045772312Y.0000000069.
- Xing, H.; Yin, H.; Sun, C.; Ren, X.; Tian, Y.; Yu, M.; Jiang, T. Preparation of an Acellular Spinal Cord Scaffold to Improve Its Biological Properties. *Mol. Med. Rep.* **2019**, *20*, 1075–1084, doi:10.3892/mmr.2019.10364.

16. Abbaszadeh, H.-A.; Tiraihi, T.; Delshad, A.R.; Saghedhi Zadeh, M.; Taheri, T. Bone Marrow Stromal Cell Transdifferentiation into Oligodendrocyte-like Cells Using Triiodothyronine as a Inducer with Expression of Platelet-Derived Growth Factor α as a Maturity Marker. *Iran. Biomed. J.* **2013**, *17*, 62–70, doi:10.6091/IBJ.11162.2013.
17. Jang, S.; Cho, H.H.; Cho, Y.B.; Park, J.S.; Jeong, H.S. Functional Neural Differentiation of Human Adipose Tissue-Derived Stem Cells Using BFGF and Forskolin. *BMC Cell Biol.* **2010**, *11*, doi:10.1186/1471-2121-11-25.
18. García-Pérez, M.M.; Martínez-Rodríguez, H.G.; López-Guerra, G.G.; Soto-Domínguez, A.; Said-Fernández, S.L.; Morales-Avalos, R.; Elizondo-Omaña, R.E.; Montes-de-Oca-Luna, R.; Guzmán-López, S.; Castillo-Galván, M.L.; et al. A Modified Chemical Protocol of Decellularization of Rat Sciatic Nerve and Its Recellularization with Mesenchymal Differentiated Schwann-like Cells: Morphological and Functional Assessments. *Histol. Histopathol.* **2017**, *32*, 779–792, doi:10.14670/HH-11-844.
19. Dash, B.C.; Xu, Z.; Lin, L.; Koo, A.; Ndon, S.; Berthiaume, F.; Dardik, A.; Hsia, H. Stem Cells and Engineered Scaffolds for Regenerative Wound Healing. *Bioengineering* **2018**, *5*.
20. Yin, H.; Jiang, T.; Deng, X.; Yu, M.; Xing, H.; Ren, X. A Cellular Spinal Cord Scaffold Seeded with Rat Adipose-Derived Stem Cells Facilitates Functional Recovery via Enhancing Axon Regeneration in Spinal Cord Injured Rats. *Mol. Med. Rep.* **2018**, *17*, 2998–3004, doi:10.3892/mmr.2017.8238.
21. Yamashita, T.; Miyamoto, Y.; Bando, Y.; Ono, T.; Kobayashi, S.; Doi, A.; Araki, T.; Kato, Y.; Shirakawa, T.; Suzuki, Y.; et al. Differentiation of Oligodendrocyte Progenitor Cells from Dissociated Monolayer and Feeder-Free Cultured Pluripotent Stem Cells. *PLoS One* **2017**, *12*, e0171947, doi:10.1371/journal.pone.0171947.
22. Fitzsimmons, R.E.B.; Mazurek, M.S.; Soos, A.; Simmons, C.A. Mesenchymal Stromal/Stem Cells in Regenerative Medicine and Tissue Engineering. *Stem Cells Int.* **2018**, *2018*, doi:10.1155/2018/8031718.
23. Zhou, Z.; Chen, Y.; Zhang, H.; Min, S.; Yu, B.; He, B.; Jin, A. Comparison of Mesenchymal Stromal Cells from Human Bone Marrow and Adipose Tissue for the Treatment of Spinal Cord Injury. *Cytotherapy* **2013**, *15*, 434–448, doi:10.1016/j.jcyt.2012.11.015.
24. Nazm Bojnordi, M.; Movahedin, M.; Tiraihi, T.; Javan, M.; Ghasemi Hamidabadi, H. Oligoprogenitor Cells Derived from Spermatogonia Stem Cells Improve Remyelination in Demyelination Model. *Mol. Biotechnol.* **2014**, *56*, 387–393, doi:10.1007/s12033-013-9722-0.
25. Ebrahimi-Barough, S.; Kouchesfahani, H.M.; Ai, J.; Massumi, M. Differentiation of Human Endometrial Stromal Cells into Oligodendrocyte Progenitor Cells (OPCs). *J. Mol. Neurosci.* **2013**, *51*, 265–273, doi:10.1007/s12031-013-9957-z.
26. Terzic, D.; Maxon, J.R.; Krevitt, L.; Dibartolomeo, C.; Goyal, T.; Low, W.C.; Dutton, J.R.; Parr, A.M. Directed Differentiation of Oligodendrocyte Progenitor Cells from Mouse Induced Pluripotent Stem Cells. *Cell Transplant.* **2016**, *25*, 411–424, doi:10.3727/096368915X688137.
27. Ehrlich, M.; Mozafari, S.; Glatza, M.; Starost, L.; Velychko, S.; Hallmann, A.L.; Cui, Q.L.; Schambach, A.; Kim, K.P.; Bachelin, C.; et al. Rapid and Efficient Generation of Oligodendrocytes from Human Induced Pluripotent Stem Cells Using Transcription Factors. *Proc. Natl. Acad. Sci. U. S. A.* **2017**, *114*, 1–10, doi:10.1073/pnas.1614412114.
28. Jang, S.; Cho, H.-H.; Cho, Y.-B.; Park, J.-S.; Jeong, H.-S. Functional Neural Differentiation of Human Adipose Tissue-Derived Stem Cells Using BFGF and Forskolin. *BMC Cell Biol.* **2010**, *11*, 25, doi:10.1186/1471-2121-11-25.
29. Ruiz-Sauri, A.; Orduña-Valls, J.M.; Blasco-Serra, A.; Tornero-Tornero, C.; Cedeño, D.L.; Bejarano-Quisoboni, D.; Valverde-Navarro, A.A.; Benyamin, R.; Vallejo, R. Glia to Neuron Ratio in the Posterior Aspect of the Human Spinal Cord at Thoracic Segments Relevant to Spinal Cord Stimulation. *J. Anat.* **2019**, *235*, 997–1006, doi:10.1111/joa.13061.
30. Kroehne, V.; Tsata, V.; Marrone, L.; Froeb, C.; Reinhardt, S.; Gompf, A.; Dahl, A.; Sternecker, J.; Reimer, M.M. Primary Spinal OPC Culture System from Adult Zebrafish to Study Oligodendrocyte Differentiation In Vitro. *Front. Cell. Neurosci.* **2017**, *11*, doi:10.3389/fncel.2017.00284.
31. Domingues, H.S.; Cruz, A.; Chan, J.R.; Relvas, J.B.; Rubinstein, B.; Pinto, I.M. Mechanical Plasticity during Oligodendrocyte Differentiation and Myelination. *Glia* **2018**, *66*, 5–14, doi:10.1002/glia.23206.
32. Furusho, M.; Ishii, A.; Bansal, R. Signaling by FGF Receptor 2 , Not FGF Receptor 1 , Regulates Myelin Thickness through Activation of ERK1 / 2 – MAPK , Which Promotes MTORC1 Activity in an Akt-Independent Manner. **2017**, *37*, 2931–2946, doi:10.1523/JNEUROSCI.3316-16.2017.

33. Singh, M.; Vaishnav, P.K.; Dinda, A.K.; Mohanty, S. Evaluation of Priming Efficiency of Forskolin in Tissue-Specific Human Mesenchymal Stem Cells. *Cells* **2020**, *9*, 1–18, doi:10.3390/cells9092058.
34. Makhija, E.P.; Espinosa-Hoyos, D.; Jagielska, A.; Van Vliet, K.J. Mechanical Regulation of Oligodendrocyte Biology. *Neurosci. Lett.* **2020**, *717*, 134673.
35. Nakada, M.; Itoh, S.; Tada, K.; Matsuta, M.; Murai, A.; Tsuchiya, H. Effects of Hybridization of Decellularized Allogenic Nerves with Adipose-Derive Stem Cell Sheets to Facilitate Nerve Regeneration. *Brain Res.* **2020**, *1746*, doi:10.1016/j.brainres.2020.147025.
36. Rbia, N.; Bulstra, L.F.; Bishop, A.T.; Van Wijnen, A.J.; Shin, A.Y. A Simple Dynamic Strategy to Deliver Stem Cells to Decellularized Nerve Allografts. *Plast. Reconstr. Surg.* **2018**, *142*, 402–413, doi:10.1097/PRS.0000000000004614.
37. Volarevic, V.; Markovic, B.S.; Gazdic, M.; Volarevic, A.; Jovicic, N.; Arsenijevic, N.; Armstrong, L.; Djonov, V.; Lako, M.; Stojkovic, M. Ethical and Safety Issues of Stem Cell-Based Therapy. *Int. J. Med. Sci.* **2018**, *15*, 36–45.
38. Porzionato, A.; Stocco, E.; Barbon, S.; Grandi, F.; Macchi, V.; De Caro, R. Tissue-Engineered Grafts from Human Decellularized Extracellular Matrices: A Systematic Review and Future Perspectives. *Int. J. Mol. Sci.* **2018**, *19*, doi:10.3390/ijms19124117.
39. Nomura, H.; Tator, C.H.; Shoichet, M.S. Bioengineered Strategies for Spinal Cord Repair. *J. Neurotrauma* **2006**, *23*, 496–507, doi:10.1089/neu.2006.23.496.
40. Philips, C.; Cornelissen, M.; Carriel, V. Evaluation Methods as Quality Control in the Generation of Decellularized Peripheral Nerve Allografts. *J. Neural Eng.* **2018**, *15*.
41. Gilpin, A.; Yang, Y. Decellularization Strategies for Regenerative Medicine: From Processing Techniques to Applications. *Biomed Res. Int.* **2017**, *2017*.
42. Agmon, G.; Christman, K.L. Controlling Stem Cell Behavior with Decellularized Extracellular Matrix Scaffolds. *Curr. Opin. Solid State Mater. Sci.* **2016**, *20*, 193–201.
43. Howard, D.; Buttery, L.D.; Shakesheff, K.M.; Roberts, S.J. Tissue Engineering: Strategies, Stem Cells and Scaffolds. *J. Anat.* **2008**, *213*, 66–72.
44. Brill, C.; Scheuer, T.; Bühner, C.; Endesfelder, S.; Schmitz, T. Oxygen Impairs Oligodendroglial Development via Oxidative Stress and Reduced Expression of HIF-1 α . *Sci. Rep.* **2017**, *7*, 1–14, doi:10.1038/srep43000.
45. Zambuto, S.G.; Clancy, K.B.H.; Harley, B.A.C. A Gelatin Hydrogel to Study Endometrial Angiogenesis and Trophoblast Invasion. *Interface Focus* **2019**, *9*, doi:10.1098/rsfs.2019.0016.
46. Lovett, M.; Lee, K.; Edwards, A.; Kaplan, D.L. Vascularization Strategies for Tissue Engineering. *Tissue Eng. - Part B Rev.* **2009**, *15*, 353–370.
47. Wang, S.; Bates, J.; Li, X.; Schanz, S.; Chandler-Militello, D.; Levine, C.; Maherali, N.; Studer, L.; Hochedlinger, K.; Windrem, M.; et al. Human iPSC-Derived Oligodendrocyte Progenitor Cells Can Myelinate and Rescue a Mouse Model of Congenital Hypomyelination. *Cell Stem Cell* **2013**, *12*, 252–264, doi:10.1016/j.stem.2012.12.002.
48. Cerqueira, S.R.; Lee, Y.S.; Cornelison, R.C.; Mertz, M.W.; Wachs, R.A.; Schmidt, C.E.; Bunge, M.B. Decellularized Peripheral Nerve Supports Schwann Cell Transplants and Axon Growth Following Spinal Cord Injury. *Biomaterials* **2018**, *177*, 176–185, doi:10.1016/j.biomaterials.2018.05.049.
49. Marquardt, L.M.; Doulames, V.M.; Wang, A.T.; Dubbin, K.; Suhar, R.A.; Kratochvil, M.J.; Medress, Z.A.; Plant, G.W.; Heilshorn, S.C. Designer, Injectable Gels to Prevent Transplanted Schwann Cell Loss during Spinal Cord Injury Therapy. *Sci. Adv.* **2020**, *6*, doi:10.1126/sciadv.aaz1039.
50. Katoh, H.; Yokota, K.; Fehlings, M.G. Regeneration of Spinal Cord Connectivity through Stem Cell Transplantation and Biomaterial Scaffolds. *Front. Cell. Neurosci.* **2019**, *13*, doi:10.3389/fncel.2019.00248.



In *Scientific Letters*, articles are published under a CC-BY license (Creative Commons Attribution 4.0 International License at <https://creativecommons.org/licenses/by/4.0/>), the most open license available. The users can share (copy and redistribute the material in any medium or format) and adapt (remix, transform, and build upon the material for any purpose, even commercially), as long as they give appropriate credit, provide a link to the license, and indicate if changes were made (read the full text of the license terms and conditions of use at <https://creativecommons.org/licenses/by/4.0/legalcode>).